A DESCRIPTION AND VALIDATION OF STEADY-STATE ANALYSIS METHODS FOR BOILING WATER REACTORS AMENDMENT 1

RESPONSE TO NRC QUESTIONS

DECEMBER 1983

APPROVED BY: B. J. Gitnick 12-22-83

B. J. Gitnick
Principal Engineer - In-Core Analysis

CAROLINA POWER & LIGHT COMPANY
411 FAYETTEVILLE STREET MALL
RALEIGH, NORTH CAROLINA 27602

INTRODUCTION

This amendment to Topical Report NF-1583.01, "A Description and Validation of Steady-State Analysis Methods for Boiling Water Reactors," is provided in response to requests for additional information as conveyed by Enclosure 3 of the letter to Mr. E. E. Utley, CP&L, from Mr. Domenic B. Vassallo, NRC Division of Licensing, dated November 1, 1983.

QUESTION 1 (NF-1583.01)

(Chapter 2)

Please provide a matrix showing a typical set of RECORD calculations which are performed in order to prepare cross-section sets for use in PRESTO-B. Include the branching calculations.

RESPONSE

A complete set of RECORD calculations for a BWR lattice are listed on the following pages. A lattice may be a distinct axial region of an assembly (for zoned fuel) or represent an entire assembly. String 3 is not repeated for lattices that differ only in Gd_2O_3 loading and String 4 is typically performed once for a lattice type, i.e., 7x7, 8x8, 8x8R.

(8688WRM/ccc)

RECORD Calculations for BWR Lattice

	T_{MOD}	T_{FUEL}
HFP	560 °K	Reference
HZP	560 °K	560 °K
CZP	292 °K	292 °K
WZP	392 °K	392 °K

Identifier: RE-Bn-11s-cc

n = BSEP Unit #

11 = Lattice # (2 digits)

s = String #

cc = Case #

String 0: Thermal Flux Ratio for JTHERMOS - Preliminary RECORD cases using generic Gd_2O_3 library to obtain thermal spectrum for Gd_2O_3 cross-section generation with JTHERMOS.

Case 00 V0 HFP ARO 0 MWD/T PIN EDIT

Case 01 V4 HFP ARO 0 MWD/T PIN EDIT

Case 02 V7 HFP ARO 0 MWD/T PIN EDIT

Case 03 V0 HZP ROD 0 MWD/T PIN EDIT

Case 04 V0 CZP ROD 0 MWD/T PIN EDIT

Case 05 V0 WZP ROD 0 MWD/T PIN EDIT

String 1: Base Cases - Cases 00-02 are depleted at constant void in 15 steps to 35 GWD/T (0, 1, 2, 3, 4, 5, 6, 7, 8, 10, 12, 15, 20, 25, 30, 35 GWD/T). The cases are restarted at each step to provide base cases for zero power conditions at different void histories, which, except for the 600 ppm cases, are rodded.

Case 00 V0 HFP ARO 0-35 GWD/T

Case 01 V4 HFP ARO 0-35 GWD/T

Case 02 V7 HFP ARO 0-35 GWD/T

Case 03 VH0 HZP ROD 0-35 GWD/T (Restart Case 00)

Case 04 VH4 HZP ROD 0-35 GWD/T (Restart Case 01)

Case 05 VH7 HZP ROD 0-35 GWD/T (Restart Case 02)

Case 06 VH0 CZP ROD 0-35 GWD/T (Restart Case 00)

Case 07 VH4 CZP ROD 0-35 GWD/T (Restart Case 01)

Case 08 VH7 CZP ROD 0-35 GWD/T (Restart Case 02)

Case 09 VH0 CZP ARO 600 PPM 0-35 GWD/T (Restart Case 00)

Case 10 VH4 CZP ARO 600 PPM 0-35 GWD/T (Restart Case 01)

Case 11 VH7 CZP ARO 600 PPM 0-35 GWD/T (Restart Case 02)

Case 12 VH0 WZP ROD 0-35 GWD/T (Restart Case 00)

Case 13 VH4 WZP ROD 0-35 GWD/T (Restart Case 01)

Case 14 VH7 WZP ROD 0-35 GWD/T (Restart Case 02)

String 2: Control Rod Model Cases - The control rod model requires restarts at three exposure points in the alternate rodded condition.

Case 00 VH0 V0 HFP ROD 0-8-15 GWD/T (Restart String 1, Case 00)

Case 01 VH4 V4 HFP ROD 0-8-15 GWD/T (Restart String 1, Case 01)

Case 02 VH7 V7 HFP ROD 0-8-15 GWD/T (Restart String 1, Case 02)

Case 03 VH0 HZP ARO 0-8-15 GWD/T (Restart String 1, Case 00)

Case 04 VH4 HZP ARO 0-8-15 GWD/T (Restart String 1, Case 01)

Case 05 VH7 HZP ARO 0-8-15 GWD/T (Restart String 1, Case 02)

Case 06 VH0 CZP ARO 0-8-15 GWD/T (Restart String 1, Case 00)

Case 07 VH4 CZP ARO 0-8-15 GWD/T (Restart String 1, Case 01)

Case 08 VH7 CZP ARO 0-8-15 GWD/T (Restart String 1, Case 02)

Case 09 VH4 CZP-TF560 ARO 0-8-15 GWD/T (Restart String 1, Case 01)

Case 10 VH4 CZP-TFHFP ARO 0-8-15 GWD/T (Restart String 1, Case 01)

Case 11 VH0 WZP ARO 0-8-15 GWD/T (Restart String 1, Case 00)

Case 12 VH4 WZP ARO 0-8-15 GWD/T (Restart String 1, Case 01)

Case 13 VH7 WZP ARO 0-8-15 GWD/T (Restart String 1, Case 02)

String 3: CR History, Doppler Defect, Samarium, and Xenon Model Cases - Refer to PRESTO Document, NF-1583.03, Sections 4.5.3, 4.3, 4.4, and 4.2.1.

Case 00 V4 HFP ARO NOGAD 0-20 GWD/T

Case 01 V4 HFP ROD NOGAD 0-20 GWD/T

Case 02 V0 HFP ARO NOGAD 0GWD/T XE-ONLY

Case 03 V4 HFP ARO NOGAD 0GWD/T XE-ONLY

Case 04 V7 HFP ARO NOGAD 0GWD/T XE-ONLY

Case 05 V4 0.5-POWER ARO NOGAD 0GWD/T XE-ONLY

Case 06 V4 HFP ARO NOGAD 10-20GWD/T RESTART BURN (Restart Case 01)

Case 07 V4 HFP ARO NOGAD 0-5-20 RESTART 0GWD/T TF-100K (Restart Case 00)

Case 08 V0 CZP ARO NOGAD 0GWD/T HFP-XE + Sm (Restart Case 00)

Case 09 V0 CZP ARO NOGAD 0GWD/T HFP-XE (Restart Case 03)

Case 10 V0 CZP ARO NOGAD 0GWD/T 0.5 POWER-XE (Restart Case 05)

Case 11 V0 CZP ARO NOGAD 0GWD/T NO-XE (Restart Case 03)

Case 12 V4 HFP ARO NOGAD 0GWD/T NO-XE (Restart Case 03)

String 4: Spacer Grid Model Cases - Three to five exposure points are chosen for restart at zero power conditions from the depletions with spacer grid. See PRESTO Document, NF-1583.03, Section 4.7

Case 00 V0 HFP ARO GRID 0-15 GWD/T

Case 01 V4 HFP ARO GRID 0-15 GWD/T

Case 02 V7 HFP ARO GRID 0-15 GWD/T

Case 03 VH0 HZP ROD GRID 0-15 GWD/T (Restart Case 00)

Case 04 VH4 HZP ROD GRID 0-15 GWD/T (Restart Case 01)

Case 05 VH7 HZP ROD GRID 0-15 GWD/T (Restart Case 02)

Case 06 VH0 CZP ROD GRID 0-15 GWD/T (Restart Case 00)

Case 07 VH4 CZP ROD GRID 0-15 GWD/T (Restart Case 01)

Case 08 VH7 CZP ROD GRID 0-15 GWD/T (Restart Case 02)

Case 09 VH0 CZP ARO GRID 600PPM 0-15 GWD/T (Restart Case 00)

Case 10 VH4 CZP ARO GRID 600PPM 0-15 GWD/T (Restart Case 01)

Case 11 VH7 CZP ARO GRID 600PPM 0-15 GWD/T (Restart Case 02)

Case 12 VH0 WZP ROD GRID 0-15 GWD/T (Restart Case 00)

Case 13 VH4 WZP ROD GRID 0-15 GWD/T (Restart Case 01)

Case 14 VH7 WZP ROD GRID 0-15 GWD/T (Restart Case 02)

String 5: Differing Void and Exposure-Weighted Void - To compute corrections when instantaneous void differs from exposure - weighted void.

Case 00 VH0 V0 HFP ARO 0-10-35 GWD/T (Restart String 1, Case 00)

Case 01 VH0 V4 HFP ARO 0-10-35 GWD/T (Restart String 1, Case 00)

Case 02 VH0 V7 HFP ARO 0-10-35 GWD/T (Restart String 1, Case 00)

Case 03 VH4 V0 HFP ARO 0-10-35 GWD/T (Restart String 1, Case 01)

Case 04 VH4 V4 HFP ARO 0-10-35 GWD/T (Restart String 1, Case 01)

Case 05 VH4 V7 HFP ARO 0-10-35 GWD/T (Restart String 1, Case 01)

Case 06 VH7 V0 HFP ARO 0-10-35 GWD/T (Restart String 1, Case 02)

Case 07 VH7 V4 HFP ARO 0-10-35 GWD/T (Restart String 1, Case 02)

Case 08 VH7 V7 HFP ARO 0-10-35 GWD/T (Restart String 1, Case 02)

QUESTION 2 (NF-1583.01)

(Table 1.0.1 (IV))

This table indicates that the RECORD - PRESTO-B code set will be used to obtain point reactivity coefficients. Please provide a description of the manner in which this is done or a reference (e.g., RETRAN) to a description which has been or will be submitted.

RESPONSE

The methods used to obtain reactivity coefficients will be described in detail in a future topical report concerning system transient evaluations.

(8688WRM/ccc)

QUESTION 3 (NF-1583.01)

(Table 5.3.1)

Please provide more details on the manner in which the calculated and measured eigenvalues are compared for the cold critical states. What adjustments are made to the measured and calculated values in order to compare them on an equal basis?

RESPONSE

PRESTO calculations of critical statepoints are performed at cold (292° K) and warm (392° K) zero-power conditions. A temperature correction to the cold zero-power eigenvalue is obtained by interpolating between the cold and warm calculations based on the actual moderator temperature at the time of the critical. All of the critical comparisons presented in Table 5.3.1 were xenon-free, with transient samarium explicitly accounted for by the code. Period corrections were based on generic curves of reactivity vs. period provided by the vendor. The corrected PRESTO critical eigenvalue is calculated by summing the individual components as follows:

$$k_{crit} = k_{cold} + \Delta k_{temp} + \Delta k_{per}$$

where the correction terms all have negative values.

(8688WRM/ccc)

QUESTION 4 (NF-1583.01)

(Page 4-2)

(a) Are boundary conditions fixed in a cycle for which there are significant variations of power and/or flow and temperature? (b) How sensitive are the boundary conditions to control rod configurations? (c) Given a set of boundary conditions, which core statepoint yields a better comparison between measured and calculated power shapes: BOC (many rods inserted) or EOC (all rods out)? Also, which statepoint gives a better eigenvalue comparison, BOC or EOC? (d) Are these differences in the boundary conditions reflected in the uncertainty analysis? (e) What range of differences are observed? (f) Are these differences included in the uncertainty analysis?

RESPONSE

A) All of the Hot Power analyses presented in NF-1583.01 were generated using a set of boundary conditions which was constant for the unit and cycle of interest. No need has been demonstrated to generate boundary conditions for unique power and/or flow and temperature conditions.

Boundary conditions are generated for the unit and cycle of interest at the following conditions:

1) Hot Full Power (based on Haling EOC Conditions)
2) Warm Zero Power (based on Haling EOC History Files)
3) Cold Zero Power (based on Haling EOC History Files)

These boundary conditions are held constant for all calculations in their respective operating range.

B) The boundary conditions have a weak dependence on the control rod configuration. In practice, this dependence is ignored except for the bottom axial node where a control rod correction is automatically applied to the thermal/fast current ratio. Figures 5.2.1 through 5.2.5 present five different control states for the same point in cycle at cold conditions. These five comparisons were generated with the same set of radial boundary conditions. For hot power conditions, the effect of control state on the boundary conditions is still small and is of little importance due to the normally low control rod inventory in the vicinity of the core periphery.

C) The comparisons shown on Figures 5.2.6 through 5.2.8 were generated based on beginning of cycle conditions with various control rod insertions. The comparison shown on Figure 4.2.2 was generated at end-of-cycle, all rods out conditions. Each of these comparisons was generated using the same set of boundary conditions. In all four cases, the peripheral bundle power prediction is as good or better than the interior bundle power predictions.

(8688WRM/cfr)

3-D TIP comparisons show no noticeable trend in prediction of the peripheral instrument responses. No noticeable trend in eigenvalue has been attributed to boundary condition effects alone.

D) All boundary condition effects are included in the uncertainties because the power, TIP, Gamma Scan and eigenvalue comparisons to measured data include the effects of any variation which may be caused by the boundary conditions.

E) The uncertainties caused by boundary condition effects have not been separated from the overall uncertainties. The 3-D comparisons to actual core operations are a product of a complex interplay between the hydraulics and neutronics. It is difficult to assign any partial variation between predicted and measured results which can be assigned to just boundary condition effects. The 2-D comparisons to fine mesh also present a composite effect of heterogeneous neutronic and boundary condition effects.

When the boundary conditions are computed, by PRESTO-B, using fine mesh fluxes and a fixed cross section set, ratios of coarse mesh to fine mesh powers show variations on the order of 1 percent average and 3 percent maximum relative difference.

F) See response D.

QUESTION 5 (NF-1583.01)

(Figure 4.2.2)

At which point into the cycle is the calculation whose results are shown in this figure made? What is the control rod pattern? What are the power and flow conditions? Is this a typical distribution?

RESPONSE

Figure 4.2.2 was based on the End-of-Full-Power Haling conditions for Brunswick 2 cycle 5. This is an all-rods-out condition at rated power and flow (see Table 5.1.1). The neutronic and hydraulic conditions are typical in so far as the Haling power distribution represents the average power shape for the cycle.

QUESTION 6 (NF-1583.01)

(Page 4.14)

What is the linearity function used to evaluate pressure loss coefficients at powers other than the rated value?

RESPONSE

Peripheral and interior form loss coefficients are evaluated at End-of-Full-Power Haling conditions based on a reference FIBWR calculation. Once determined, these parameters remain constant throughout any given operating cycle, regardless of power or flow conditions.

(8688WRM/ccc)

QUESTION 7 (NF-1583.01)

(Page 4.14)

Are (a) pressure loss coefficients, (b) flow splits evaluated when a control rod pattern is changed? How often are flows revised? What are the criteria for revisions or updates?

RESPONSE

The bypass flow fraction in PRESTO-B is currently specified as a function of core flow. Individual bundle flows are re-allocated with each power-void iteration based on the requirement of equal pressure drop across all channels. While individual bundle flows may vary with changes in control rod pattern, or with the power distribution in general, the basic thermal-hydraulic parameters used to calculate them, namely the pressure loss coefficients and bypass flow fit coefficients, remain constant for a unit and cycle regardless of power or flow conditions.

(8688WRM/ccc)

QUESTION 8 (NF-1583.01)

(Page 4.14)

Which of the two methods for calculating bypass flows are used in (a) core follow, (b) predictive, (c) Haling calculation? What determines the choice of method? Is one method more accurate than the other? Does either of the methods account for voiding in the bypass region?

RESPONSE

In all of the PRESTO-B work presented in NF-1583.01, bypass flow fractions were calculated by applying an inlet loss coefficient to the bypass region. As in the case of peripheral and interior in-channel loss coefficients, once determined, the bypass region loss coefficient remained fixed throughout a given cycle, regardless of power or flow conditions.

Voiding in the bypass region is modeled in PRESTO-B regardless of the method used for calculating the bypass fraction. It is CP&L's intention to use the bypass region loss coefficient to calculate bypass fractions for all future design studies.

Results of PRESTO-B calculations performed using the bypass region loss coefficient and calculations performed using a fit of bypass fraction to total core flow have shown very little difference over the useful range of flows, i.e., 50 percent to 100 percent of rated. There is no evidence that either one gives more accurate results than the other.

Use of a bypass region loss coefficient has given very consistent results as shown by the PRESTO-B benchmark results in general and by the off-nominal comparisons presented in Figures 5.5.21-30 and Table 5.8.1 in particular.

(8688WRM/cfc)

QUESTION 9 (NF-1583.01)

(Section 4.4)

What criteria are used to determine whether the iterative power distribution exposure procedure should be employed when core conditions are changing? What is the maximum change in reactor power, flow, control rod insertion, etc., between the beginning and end of the exposure interval? What are the bases for the criteria?

RESPONSE

The PRESTO iterative depletion feature is used when: for a given control rod pattern, the core power level or the core flow changes significantly between the beginning and the end of the depletion step; for a given basic control rod configuration, when there are significant changes in the individual control rod insertions; or when the depletion step is sufficiently long that the end-of-step power distribution changes noticeably due to the effects of the depletion itself.

Typically, changes in core power or flow of more than 5 percent, rod insertion changes of more than 2 notches on two or more control rods, or depletion steps of greater than 500 MWD/MT warrant the use of the iterative depletion.

The application of these criteria is somewhat subjective, in that the criteria are guidelines attempting to quantify the deviation from static conditions necessary for the iterative method to show a significant difference than the standard depletion technique.

QUESTION 10 (NF-1583.01)

(Section 5.1)

Please provide power and flow histograms for a typical cycle that was used in the verification data base.

RESPONSE

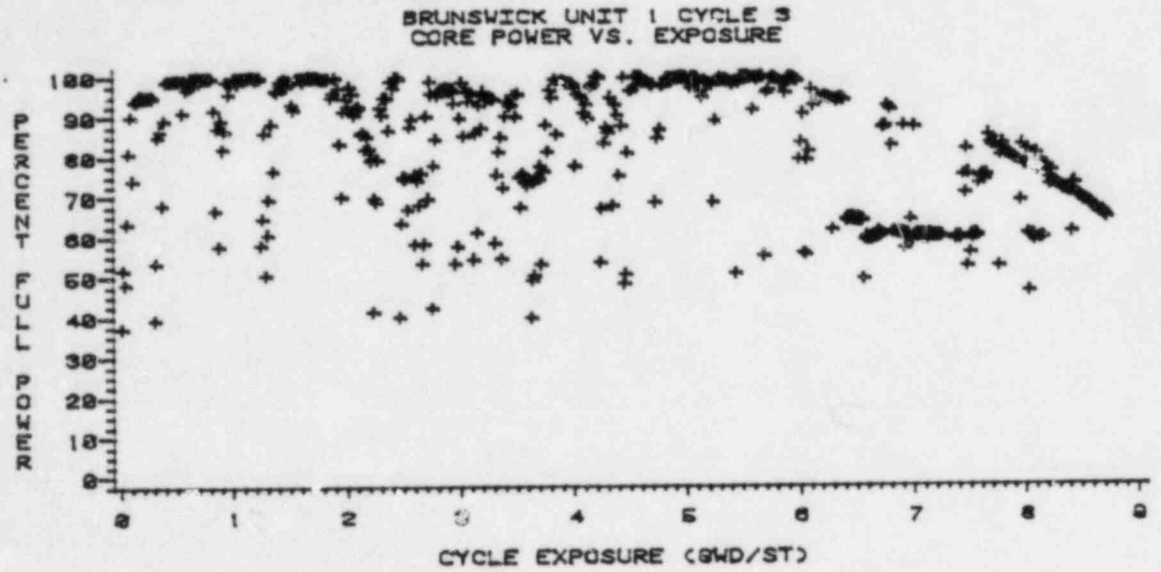

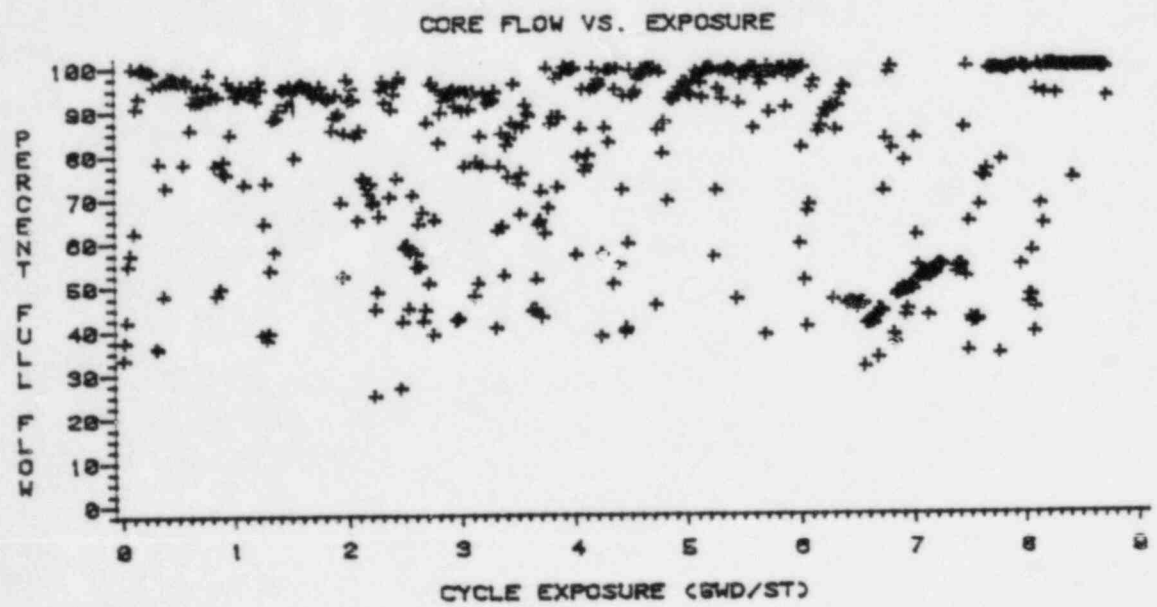

(8688WRM/ccc)

QUESTION 11 (NF-1583.01)

(Section 5.5)

Please provide data showing PRESTO-TIP comparisons for individuals TIPS. Data similar to that shown in the March 11, 1982 meeting will suffice if legibility can be improved. Alternately, choose several individual traces representing different control rod insertions and time in cycle.

RESPONSE

Included are multiple TIP plots for each Brunswick cycle presented in NF-1583.01, each showing thirty-one individual TIP traces. Figures 11.1 through 11.9 show different control rod insertions for each cycle, as indicated in Table 5.5.1 of NF-1583.01. Four sets of full-size copies are enclosed for detailed inspection.

Figure 11.1

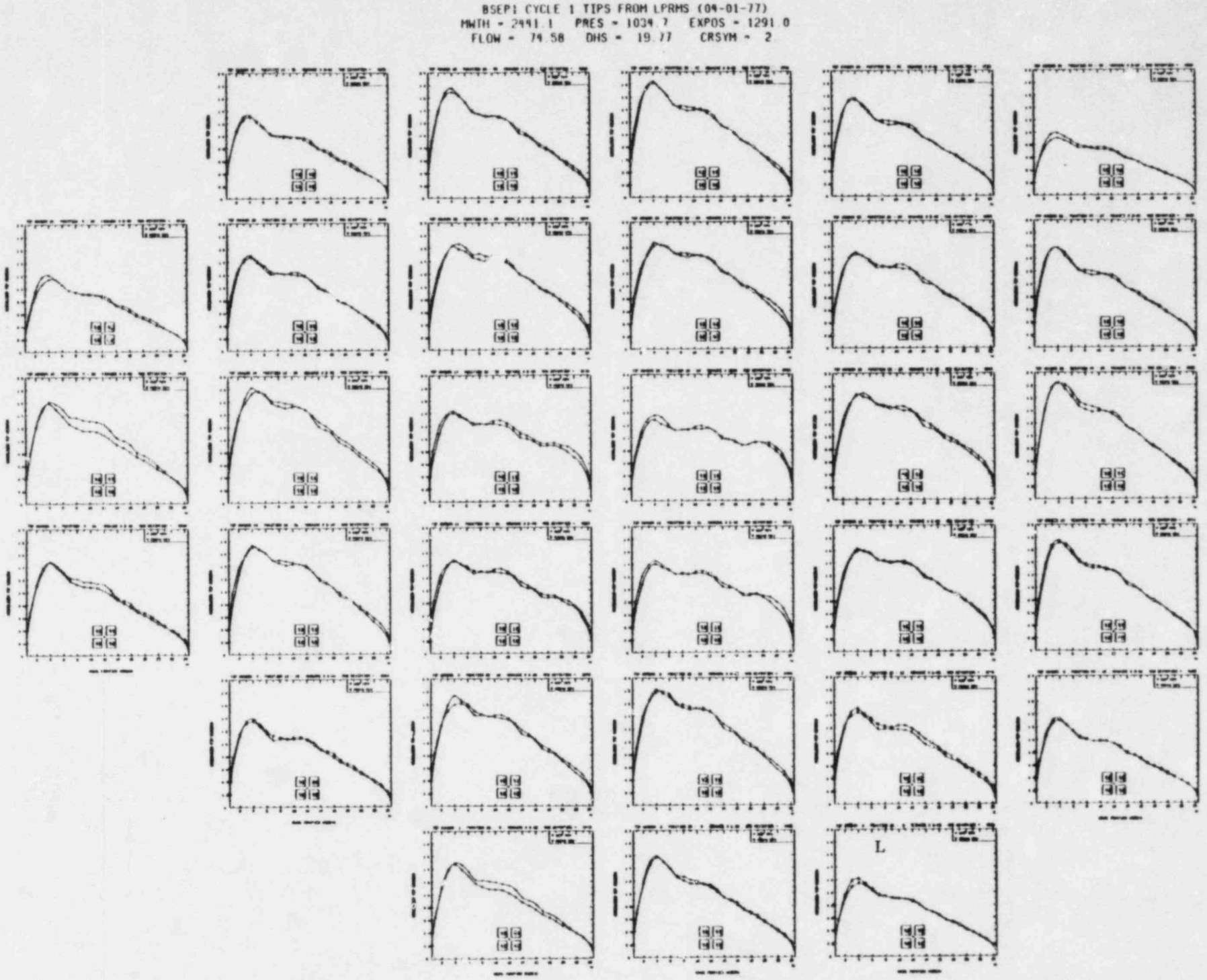
BSEP1 CYCLE 1 TIPS FROM LPRMS (04-01-77)
MWTH = 2991.1 PRES = 1034.7 EXPOS = 1291.0
FLOW = 74.58 DHS = 19.77 CRSYM = 2
L

Figure 11.2

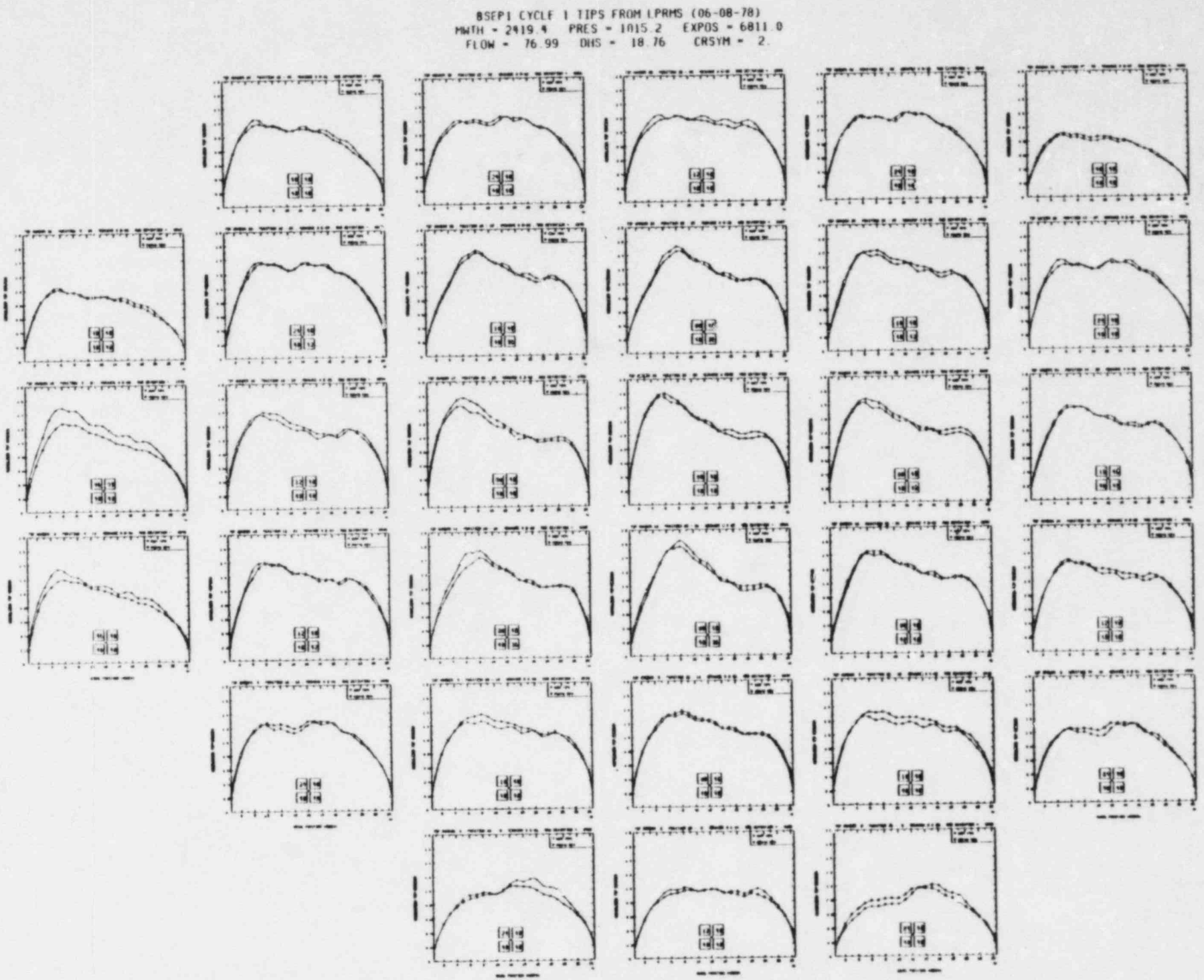
BSEP1 CYCLE 1 TIPS FROM LPRMS (06-08-78)
MWTH = 2919.9 PRES = 1015.2 EXPOS = 6811.0
FLOW = 76.99 DHS = 18.76 CRSYM = 2.

Figure 11.3

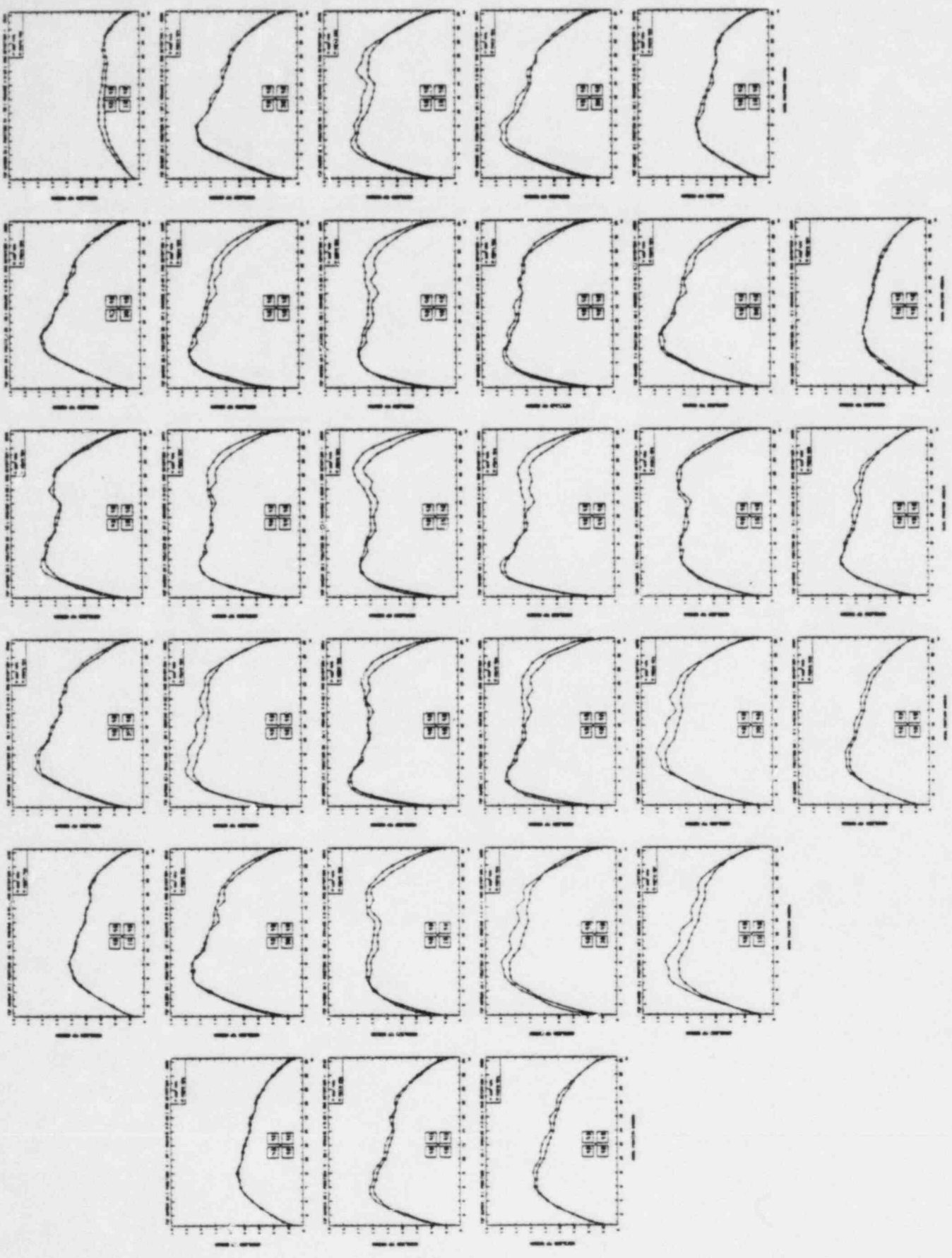
BSEP1 CYCLE 2 TIPS FROM LPRMS (02-26-80)
MWTH = 2439.9 PRES = 1016.3 EXPOS =12027.0
FLOW = 73.76 DHS = 19.91 CRSYM = 2.

Figure 11.4

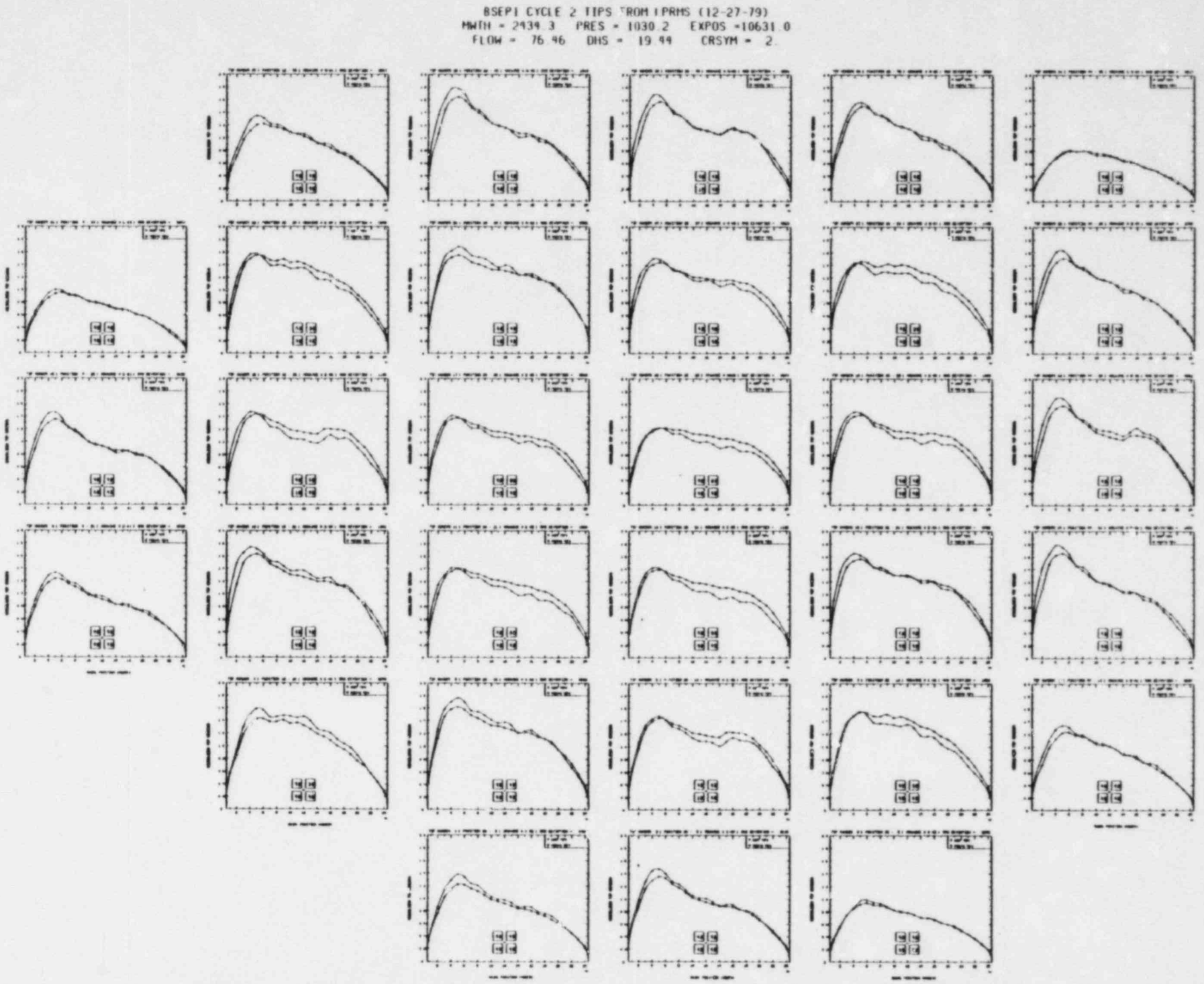
BSEPI CYCLE 2 TIPS FROM IPRMS (12-27-79)
MWTH = 2939.3 PRES = 1030.2 EXPOS =10631.0
FLOW = 76.96 DHS = 19.99 CRSYM = 2

Figure 11.5

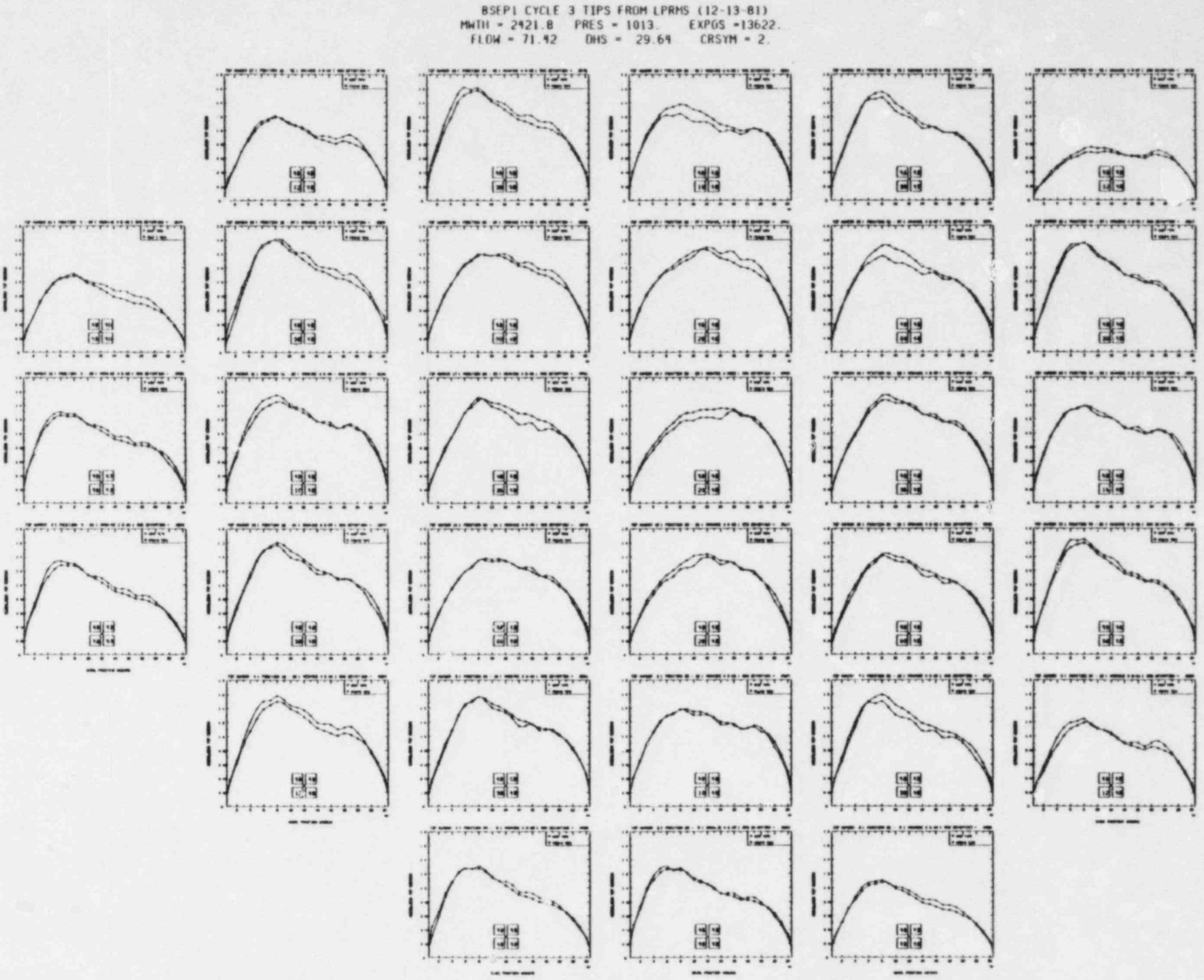
BSEP1 CYCLE 3 TIPS FROM LPRMS (12-13-81)
MWTH = 2421.8 PRES = 1013. EXPOS =13622.
FLOW = 71.42 DHS = 29.69 CRSYM = 2.

Figure 11.6

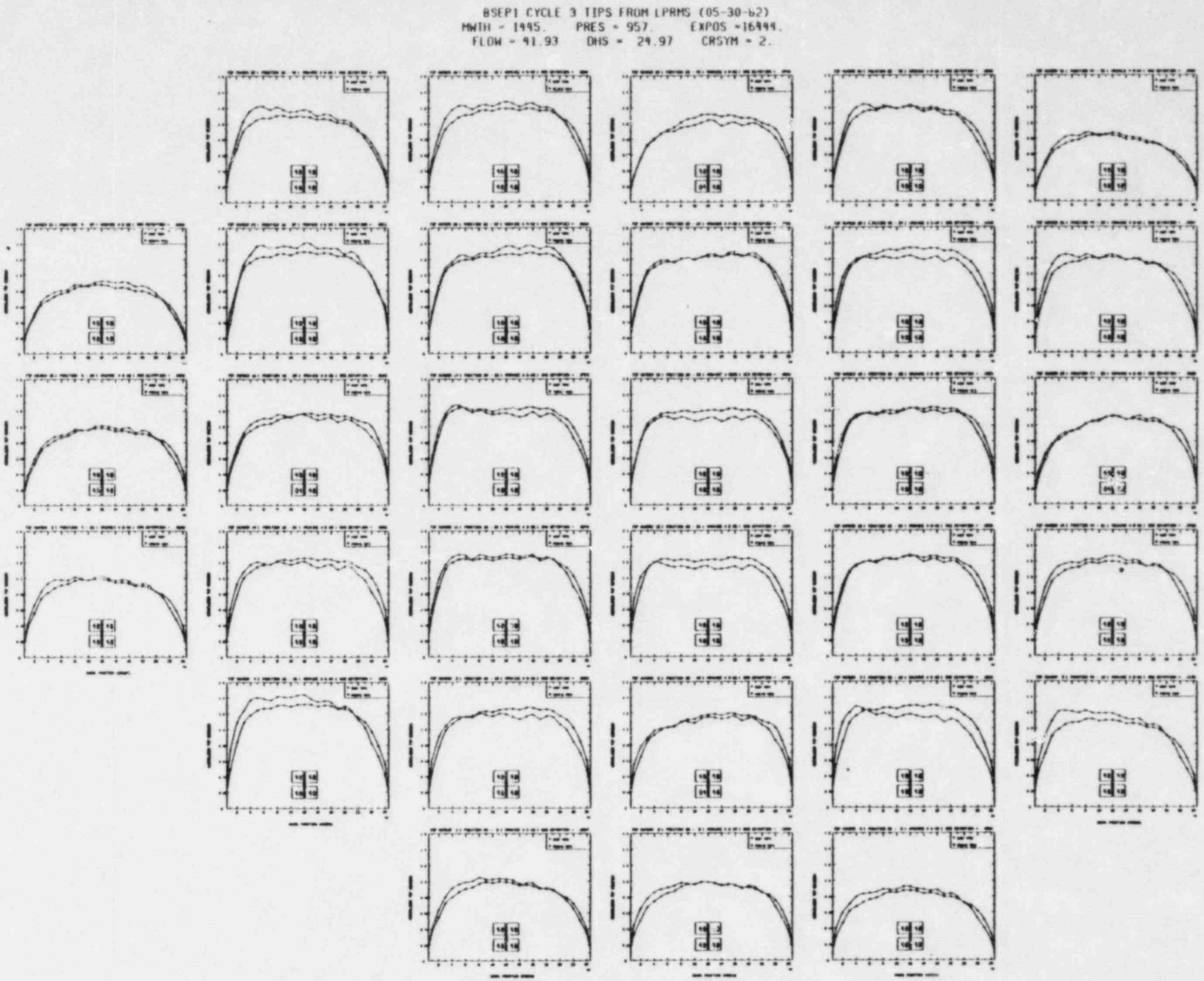
BSEP1 CYCLE 3 TIPS FROM LPRMS (05-30-92)
MWTH = 1995. PRES = 957. EXPOS =16999.
FLOW = 91.93 DHS = 29.97 CRSYM = 2.

Figure 11.7

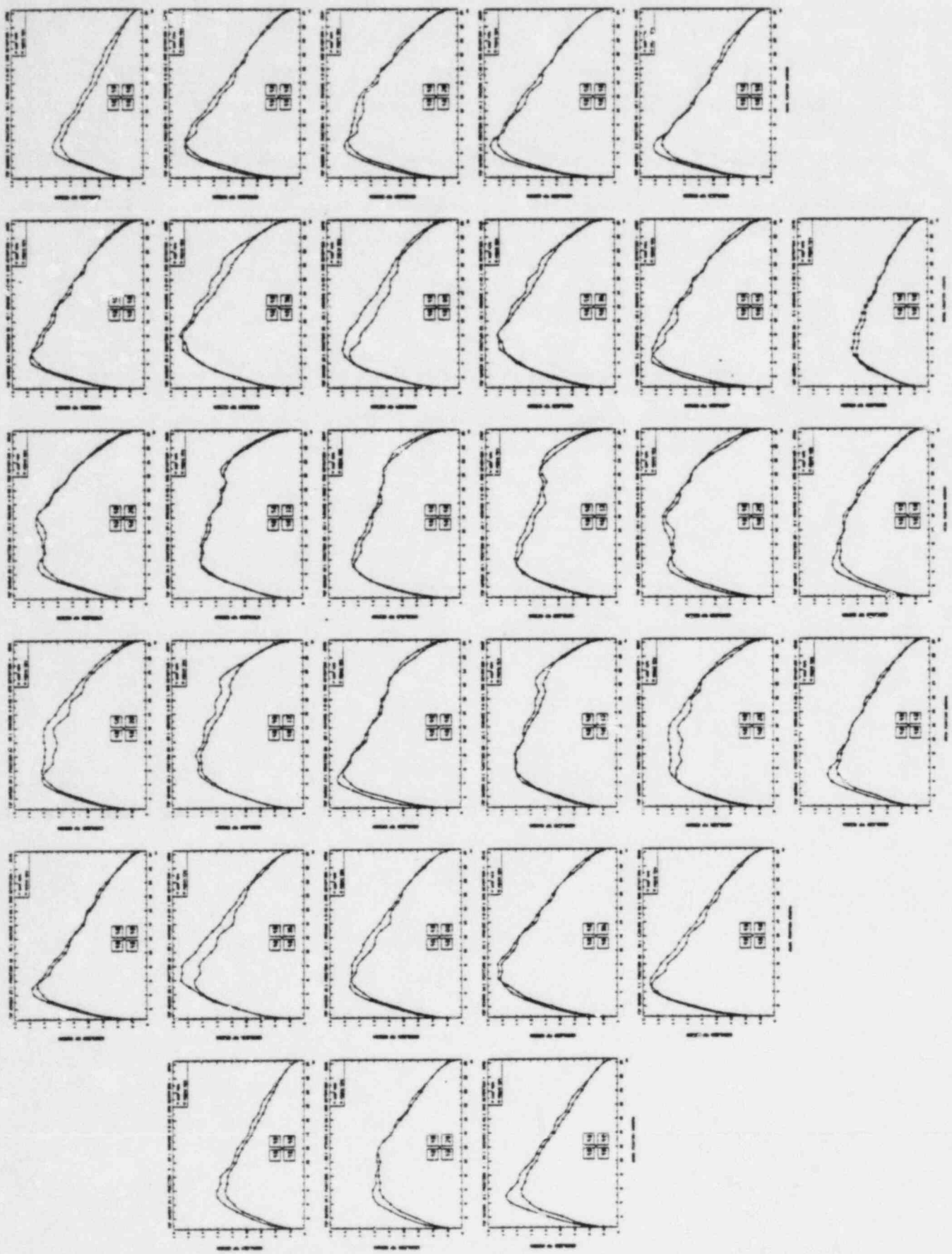
BSEP2 CYCLE 9 TIPS FROM LPRMS (10-25-80)
MWTH = 2382.3 PRES =1019.8 EXPOS = 9878.1
FLOW = 74.17 DHS = 20.98 CRSYM = 2.

Figure 11.8

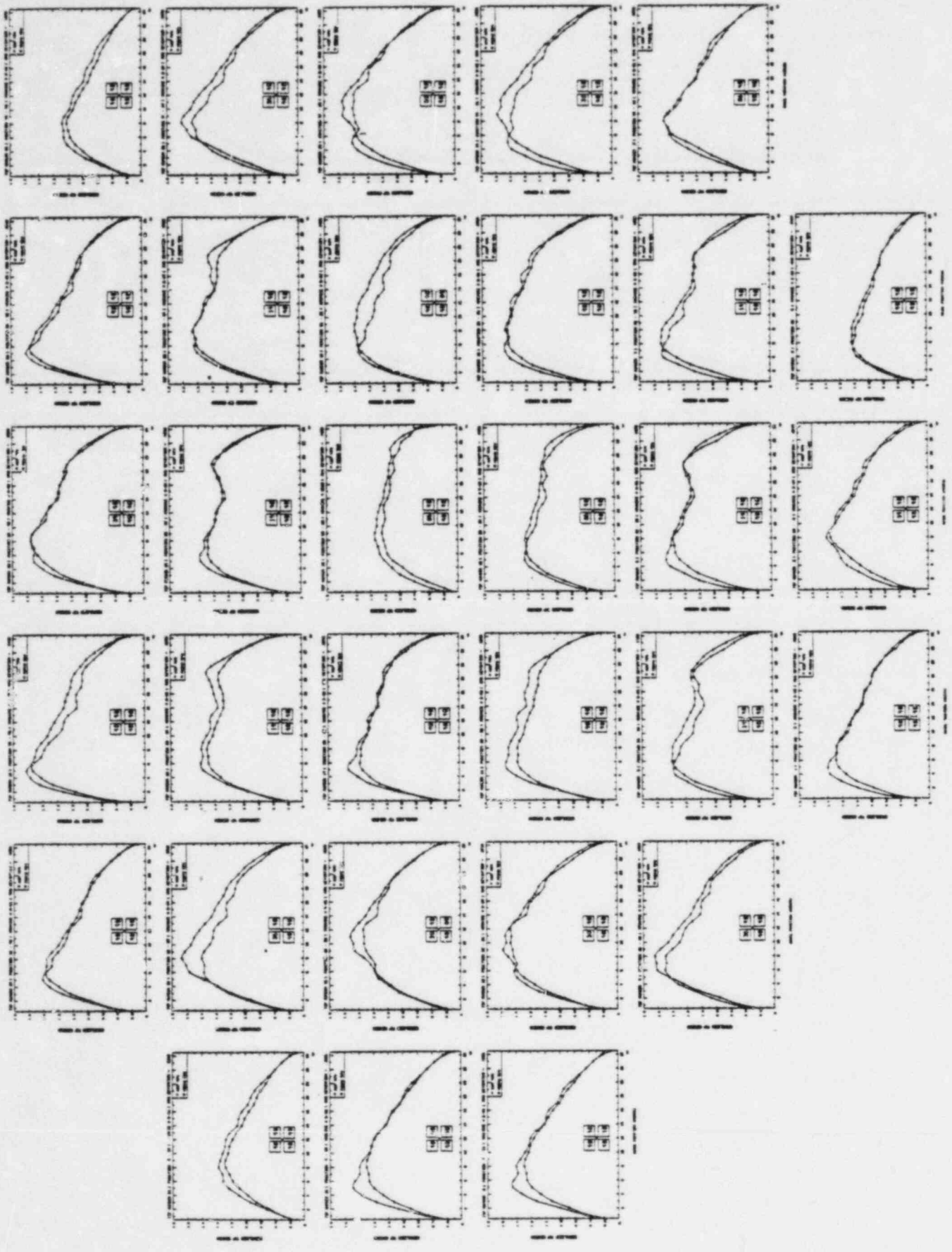
BSEP2 CYCLE 9 TIPS FROM LPRMS (04-30-81)
MWTH = 2373.0 PRES =1018.0 EXPOS -11841.0
FLOW = 72.86 DPS = 20.56 CRSYM = 2.

Figure 11.9

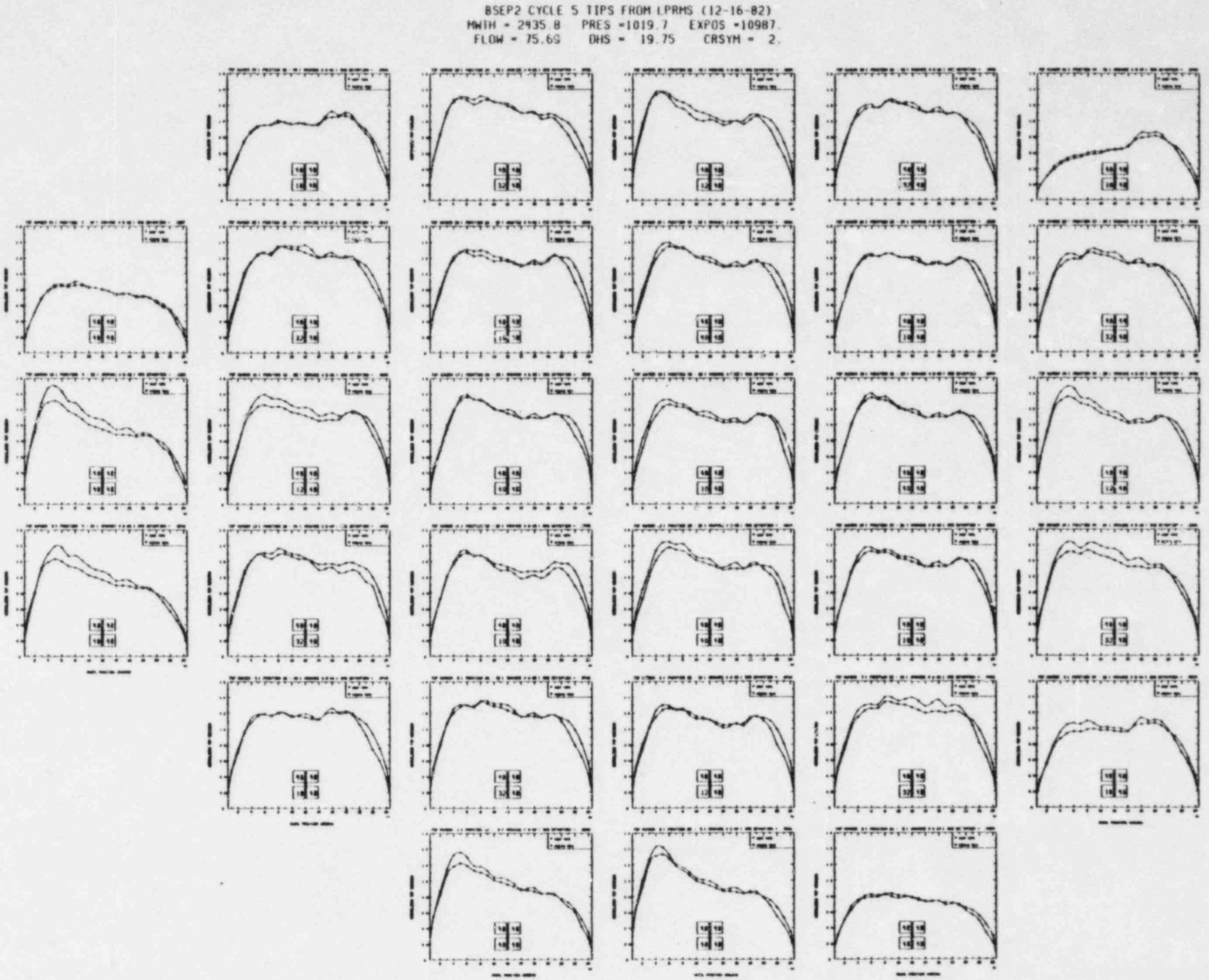
BSEP2 CYCLE 5 TIPS FROM LPRMS (12-16-82)
MWTH = 2435.8 PRES =1019.7 EXPOS =10987.
FLOW = 75.6G DHS = 19.75 CRSYM = 2.

QUESTION 12 (NF-1583.01)

(Table 5.5.1)

Are the comparisons shown in this table performed on all TIPS at the indicated statepoints? Are the comparisons typical of those for dates not shown?

RESPONSE

The TIP comparison data presented in Table 5.5.1 of NF-1583.01 takes into account all 31 individual TIP strings for each case presented. The major criteria in the choice of comparisons to be presented were their equilibrium steady-state conditions and their close proximity to a process computer OD-1 TIP recalibration. Measured process computer TIPs are back-calculated from LPRM readings. Therefore, cases containing a large number of 'blip' corrections (process computer corrections for control rod moves following an OD-1) or with obviously drifting LPRM's were not included. In selecting the cases to be presented, the goal was to present the best quality measured data, and not necessarily the best predicted vs. measured comparisons.

(8688WRM/ccc)

QUESTION 13 (NF-1583.01)

(Table 5.6.1)

The data shown are direct comparisons between measurement and calculation. Are the uncertainties shown to be used as the calculational uncertainties (i.e., the measurement uncertainties assumed to be nil)?

RESPONSE

The results in Table 5.6.1 are included only for comparison to the complete eighth-core set shown in Table 5.6.2. An axial peaking factor is not directly included in the definitions of MFLPD* or MAPLHGR** so its uncertainty is not directly applicable. The uncertainty is included in the core-wide nodal standard deviation of 3.77% shown in Figure 5.6.4 based on direct comparisons between measurement and calculation. As shown in Figure 6.3.1, this is combined with the reported measurement standard deviation of 2.5% to give the 1σ for PRESTO nodal power of 4.5%; this corresponds to the 1σ uncertainty in PRESTO predicted MAPLHGR. The 1σ uncertainty in PRESTO predicted MFLPD is 5.7%, the combination of nodal and local peak uncertainty where measurement uncertainty is included in the derivation of each.

---

* MFLPD - Maximum Fraction of Limiting Power Density.

** Maximum Average Planer Linear Heat Generation Rate.

QUESTION 14 (NF-1583.01)

With respect to the reload analyses:

a. What is used as the target cold clean eigenvalue?
b. What value is used for the target hot eigenvalue. Is the value cycle dependent? What is its uncertainty?

RESPONSE

Based on the data presented in NF-1583.01,

a. the target cold clean eigenvalue to be used in reload analyses is 0.9950, with a standard deviation of 0.002; and
b. the target hot eigenvalue is 0.9956, with a standard deviation of 0.002.

These values are for reload cycles and are not cycle dependent. We do, however, intend to monitor critical eigenvalues on a continuing basis as new benchmark data becomes available. Should any significant trends in critical eigenvalue become apparent, they will be incorporated into subsequent design analyses along with appropriate statistical conservatisms.

DOCUMENT/ PAGE PULLED

ANO. 8401130257

NO. OF PAGES 9

REASON

☐ PAGE ILLEGIBLE
☐ HARD COPY FILED AT: PDR CF
OTHER

☐ BETTER COPY REQUESTED ON

☒ PAGE TOO LARGE TO FILM
☒ HARD COPY FILED AT: PDR (CF)
OTHER

☐ FILMED ON APERTURE CARD NO 8401130257-01

thru 09